Spatiotemporal assessment of snowstorm resilience: a case study in Northeast China

Natural Hazards (2025) 121:20147–20170
https://doi.org/10.1007/s11069-025-07591-8

ORIGINAL PAPER

Spatiotemporal assessment of snowstorm resilience: a case study in Northeast China

Peijun Lu[1] · **Yicheng Wang**[2]

Received: 5 November 2024 / Accepted: 8 August 2025 / Published online: 2 September 2025

Abstract

With global warming, the frequency and intensity of snowstorms have increased, posing significant risks for high-latitude regions in Northeast China, where underdeveloped infrastructure and high vulnerability amplify these threats. This study introduces an indicator-based framework for quantitatively assessing snow resilience, grounded in the Hazard-Exposure-Vulnerability-Adaptation (HEVA) model. Applied across Heilongjiang, Jilin, and Liaoning provinces, the framework captures resilience patterns from 2005 to 2020 using geostatistical analysis and machine learning techniques. Results reveal a strong correlation between snow resilience and snow hazard losses, validating the framework's effectiveness in snow disaster management for high-risk areas. Spatial distribution patterns indicate hot and cold resilience spots, reflecting variations in vulnerability, exposure, and adaptive capacity across regions over time. The framework's machine learning clustering approach further classifies resilience characteristics, while a Gradient Boosting Machine (GBM) analysis identifies infrastructure density, grassland extent, and transportation networks as key resilience-enhancing factors. Findings underscore the critical role of well-developed infrastructure in mitigating snow hazard impacts and enhancing adaptive capacity, offering targeted insights for resilience-building interventions. This study addresses a crucial research gap by providing a systematic, spatiotemporal approach to understanding resilience in snowstorm-prone regions. Its results support policymakers in disaster reduction planning and highlight the interconnected roles of social, environmental, and infrastructural elements in resilience. The framework contributes a robust model for global application, facilitating enhanced preparedness and adaptation strategies in regions increasingly vulnerable to intensified snow hazards due to climate change.

Highlight

• A comprehensive framework evaluates snowstorm resilience across spatial and temporal dimensions.
• The framework's effectiveness is validated through real snow disaster losses in a case study.
• Advanced machine learning reveals spatiotemporal resilience pattern and key influencing factors.
• Well-developed infrastructure and extensive green space enhance resilience to snowstorms.

Extended author information available on the last page of the article

Graphical Abstract

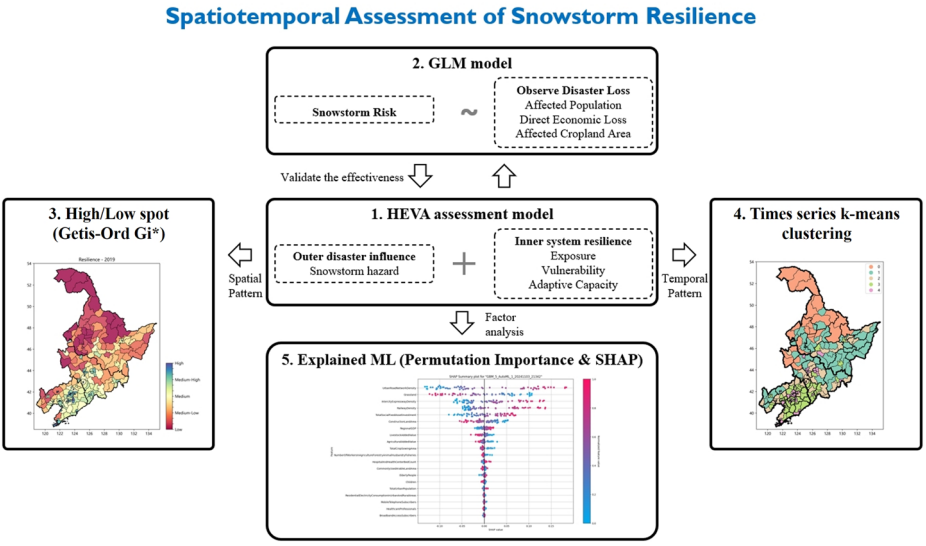

Keywords Resilience assessment · Snow disaster · Spatiotemporal analysis · Machine learning · Influence factors

1 Introduction

The warming of Earth's climate does not imply that every region experiences uniformly higher temperatures throughout the year. While the cryosphere is shrinking, cryospheric hazards are expected to intensify as the climate warms (Ding et al. 2021). Rapid atmospheric warming and sea ice loss in the Arctic are projected to shift weather system trajectories, increasing both the intensity and duration of snowfall and rainfall events, often accompanied by significantly higher wind speeds. These intensified patterns threaten ecosystems, communities, and economies. (Parker et al. 2022). Furthermore, evidence from Europe indicates that climate change will generally lead to an increase in severe winter weather events, particularly across the temperate latitudes of the Northern Hemisphere (Miller 2021). In North America, regions have seen heightened snowfall event intensity, exceeding historical thresholds, with increased cold-related mortality over the past few decades (Conroy 2023; Liu et al. 2025; Musselman et al. 2018; Quante et al. 2021). Regional climate models predict that, with global mean temperatures rising 2 °C above pre-industrial levels, Japan will experience more frequent heavy daily snowfall events (Kawase et al. 2020).

The mid- to high-latitudes of the Northern Hemisphere have witnessed an increase in extreme snow events (Walsh et al. 2020), underscoring the urgent need to strengthen resilience against heavy snow-related disasters. In contrast to resilience frameworks developed for other hazards—such as floods, heatwaves, and earthquakes (Freddi et al. 2021a, b; Fu et al., 2024; Morrison et al. 2018) —snow disaster resilience has received limited empirical attention and remains in its early stages.

Current studies on resilience to snow disasters have primarily explored temporal variations within specific urban subsystems. For instance, Mirjalili et al. (2023) conducted a quantitative analysis of New York City's transportation network during a snowstorm, using heuristic network metrics to capture the system's temporal dynamics. Similarly, Santiago-Iglesias et al. (2023) applied a spatiotemporal analysis based on Google Popular Times data to assess urban vulnerability and resilience in Madrid during a major snowfall in January 2021. Other research has focused on power system disruptions, emphasizing operational strategies to manage the real-time impacts of extreme weather (Carlini et al. 2019).

Current research on methodologies for studying resilience to snow disasters primarily utilizes network analysis and model-based simulations. In traffic network studies, for example, graph theory-based network analysis has been applied to evaluate traffic resilience during snow events (Mirjalili et al. 2023). Similarly, Wang and Liu (2019) propose a resilience-based evacuation method for urban road networks, using a tabu search algorithm to solve the location-allocation problem during extreme snow events. In another study, researchers in Italy developed a simulation model for physical power infrastructure, identifying vulnerable power line subcomponents and calculating outage return intervals (Pitto et al. 2019). These models provide in-depth insights into urban subsystem responses to disruptions, often integrating algorithms to accelerate response times and enhance overall system resilience.

Despite these advancements, significant gaps remain in snow resilience research. Most studies focus on individual urban subsystems and short timeframes, typically analyzing single events, which limits the generalizability of findings. Furthermore, research predominantly targets specific cities, making broader applications challenging due to varying urban conditions. This highlights the need for a systematic spatiotemporal assessment of snow disaster resilience across both temporal and spatial dimensions. Such an assessment is crucial for informed decision-making, particularly as regions in the northern mid- to high-latitudes face increasingly severe, yet underexplored, snow-related hazards. In Northeast China's mid- to high-latitude regions, two primary factors contribute to the frequent and severe occurrence of snowstorm hazards. First, severe snowstorms, often accompanied by strong winds and low temperatures, regularly impact both urban and rural areas. The geographic and climatic conditions of Northeast China make it particularly susceptible to these events (D. Liu et al. 2020). Second, the pace of urbanization in Northeast China lags behind the national average (J. Xu et al., 2020), with underdeveloped infrastructure, a relatively weak healthcare system, and a lower proportion of highly educated individuals (Ma et al., 2020; T. Shi et al., 2022). This disparity reduces the adaptive capacity of high-latitude areas, increasing their susceptibility to intensified snowstorm impacts. As a result, mitigating these impacts, enhancing snowstorm resilience, and identifying critical determinants of resilience are essential for revitalizing Northeast China.

This study presents a quantitative and flexible framework to evaluate snow hazard resilience. By analyzing the temporal and spatial variations of resilience in Northeast China from 2005 to 2019, this research provides a detailed understanding of how urban systems have adapted to and managed these hazards over time. Additionally, it identifies time-series patterns to elucidate resilience trends and determine key influencing factors. Through this analysis, we aim to contribute a robust knowledge base for understanding snow disaster resilience in mid- to high-latitude regions.

2 Materials and methods

2.1 Research area

This study was conducted in Northeast China, encompassing Heilongjiang, Jilin, and Liaoning provinces (Fig. 1), which shares borders with North Korea and Russia and is situated between 118°53' – 135°05' E and 38°43' – 53°33' N in the mid- to high-latitudes. Spanning an area of 809,100 km² and comprising 34 cities, Northeast China features diverse topography, with hilly mountains to the east and plains to the south. The region experiences a temperate monsoon climate with pronounced seasonal variations, leading to long, severe winters heavily influenced by the Siberian High. Winters average −10 °C to -20 °C, with 200–500 mm of snowfall annually. According to the Provincial Meteorological Bureaus and Climate Centres of Heilongjiang, Jilin, and Liaoning, snow hazards caused direct economic losses totally 898 million CNY from 2011 to 2020.

2.2 Data sources

The data sources for this study encompass diverse spatial and temporal resolutions essential for evaluating various dimensions of resilience to snow hazards (Table 1). Land-Use and Land-Cover Change data, reflecting shifts from 2005 to 2020, were obtained from the Resource and Environment Data Cloud Platform (https://www.resdc.cn) with a 30-meter resolution.

Snowfall data from 2005 to 2019 were sourced from the daily snow water equivalent product available at the National Cryosphere Desert Data Centre (J. Wang and Liu 2019). Additional meteorological data, including daily minimum temperature, maximum daily wind speed, and minimum daily relative humidity, were collected from the daily meteorological dataset of basic meteorological elements of the China National Surface Weather Station (https://data.cma.cn/). Socio-economic data—encompassing economic, employme

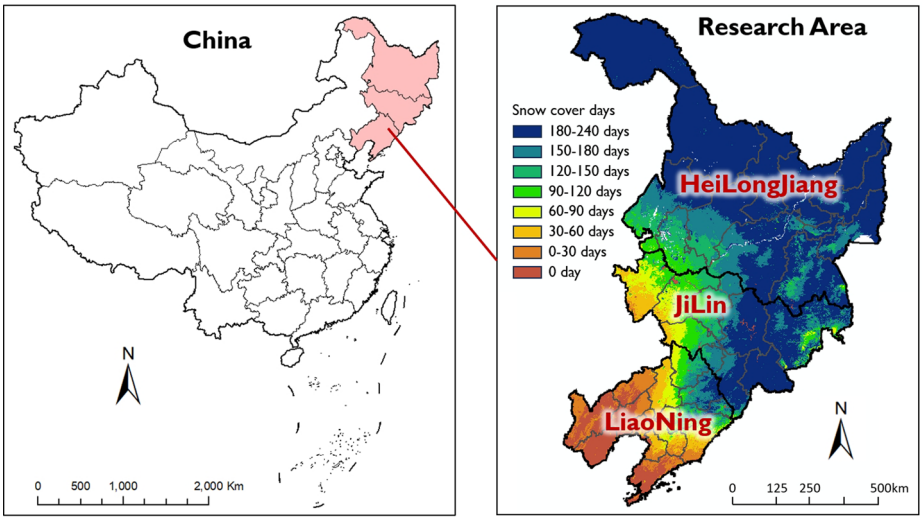

Fig. 1 Map of the study area in Northeast China, showing Heilongjiang, Jilin and Liaoning provinces with snow cover days distribution

Table 1 Data sources used in the study, including types, descriptions, and resolutions

No	Data type	Description	Source
1	Land-Use and Land-Cover Change	2005,2010,2015,2018,2020 land-use and land-cover	https://www.resdc.cn
2	Snowfall	Daily snow depth and water equivalent product from 2005 to 2019 over China.	https://www.ncdc.ac.cn/
3	Temperature, Speed, Relative Humidity	Daily minimum temperature, maximum daily wind speed and minimum daily relative humidity from 2005 to 2019 over China	https://data.cma.cn/
4	Social economy	Economy, employment, and utility infrastructure data from 2000 to 2019	Heilongjiang, Jilin and Liaoning County Statistical Yearbook and City Statistical Yearbook
5	Population data	National census (5th, 6th, 7th)	https://www.stats.gov.cn/
6	Traffic networks	Guodao, Shengdao, highway, primary, secondary, and other roads	https://www.openstreetmap.org

nt, and infrastructure statistics from 2005 to 2019—were sourced from the County and City Statistical Yearbooks for Heilongjiang, Jilin, and Liaoning provinces. Population data from the fifth through seventh national censuses were accessed through the National Bureau of Statistics of China (https://www.stats.gov.cn/). Finally, comprehensive traffic network information, covering road types from national highways to local roads, was gathered from OpenStreetMap (https://www.openstreetmap.org/).

2.3 Spatiotemporal indicator-based assessment framework

We propose an indicator-based framework to assist policymakers and urban planners in assessing, enhancing, and monitoring resilience across space and time. The framework (Fig. 2) is structured into five key components:

- Part 1: Snowstorm resilience assessment, based on the Hazard-Exposure-Vulnerability-Adaptation (HEVA) model, forms the core of the framework. This is the framework's core component.
- Part 2: An Generalized Linear Modeling (GLM) model is employed to validate the effectiveness of Part 1 using observed disaster loss data.
- Parts 3 and 4: Advanced algorithms are used to analyse and identify hot and cold resilience spatial spots patterns and temporal clustering patterns.
- Part 5: A supervised machine learning model with explainable features is applied to identify the key drivers of snowstorm resilience.

2.4 Hazard-Exposure-Vulnerability-Adaptation (HEVA) assessment model

2.4.1 Assessment models for snowstorm risk and resilience

This study quantifies snowstorm risk and resilience by evaluating both losses and system performance within urban environments. Snowstorm risk (denote as S_{Ri}) is assessed based on the impact of hazards on the system(Shah et al. 2020). Defined as a snowstorm with

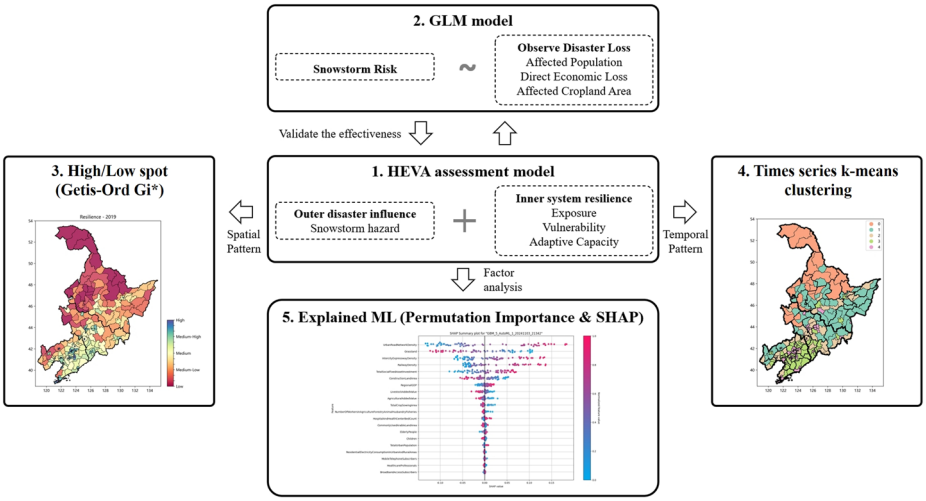

Fig. 2 A comprehensive, indicator-based framework for spatiotemporal snowstorm assessment using HEVA, GLM, and machine learning models

specific effects on population and service provision, snowstorm risk is calculated using the formula:

$$SRi = SH \times E \times V / A$$

Where, *SH* represents the snow hazard, which can cause losses in life, health, economy, or the environment; *E* denotes exposure, referring to people, property, systems, or other elements within snow hazard zones, thus subject to potential losses; *V* indicates vulnerability, reflecting the characteristics that make a community, system, or asset susceptible to snow hazards; *A* signifies adaptive capacity, or the adjustments made within natural or urban systems in response to actual or anticipated climatic stimuli, aiming to reduce harm or exploit potential benefits.

According to complex adaptive systems theory (Shi et al. 2021), snow hazards are considered external environmental shocks to the urban system, with the remaining factors reflecting the urban complex system's resilience to such hazards. Accordingly, this study defines snowstorm resilience (denoted as S_{Re}) as:

$$SRe = A / E \times V$$

2.4.2 Assessment indicators for snowstorm risk and resilience

We use a multi-dimensional set of indicators to evaluate snowstorm risk and resilience. Given the lack of established frameworks specific to snowstorm resilience, indicator selection draws on existing frameworks for other hazards, such as floods, heatwaves, and earthquakes (Dong et al. 2020; Liu et al. 2020; Shah et al. 2020; Zhao and Sun 2021). Additionally, the indicators reflect practical priorities in snow disaster management, where

communication access (He et al. 2024), healthcare capacity (Salas et al. 2024), and transportation infrastructure (Haeberli and Whiteman 2021) are central to emergency response.

Table 2 outlines the dimensions, first-level indicators, second-level indicators, and corresponding references used in this study:

2.4.3 Weighting method

To ensure robust and unbiased indicator evaluation across the HEVA framework, we adopt a hybrid weighting strategy that combines empirically derived weights for hazard classification and entropy-based weights for the remaining dimensions (exposure, vulnerability, and adaptive capacity).

For the snow hazard (SH) dimension, we use weights specified in the Chinese national meteorological guideline "Meteorological Grades for Urban Snow Hazard" (GB/T40239—2021) (China Meteorological Administration 2021), issued by the China Meteorological Administration. This empirical method assigns fixed weights to core snowstorm indicators (e.g., accumulated snowfall, snow depth, consecutive snow days, wind speed, minimum temperature, and relative humidity) based on expert knowledge and historical meteorological impact studies. This standard-based approach reduces uncertainty in the classification of snow hazard intensity and ensures comparability with national risk grading practices.

For the exposure (E), vulnerability (V), and adaptive capacity (A) dimensions, we apply the entropy weighting method, which is objective and fully data-driven. This method calculates indicator weights based on the degree of variation and information content across the dataset. Greater variability in an indicator leads to higher assigned weight, reflecting its stronger influence in distinguishing resilience levels across spatial units. To accommodate the temporal nature of our data, an exponential decay model is used to adjust weights over time, ensuring consistency in dynamic assessments.

This mixed approach improves the robustness of the overall assessment: the empirical weightings anchor the hazard evaluation to authoritative national knowledge, while the entropy weightings minimize subjectivity in measuring the socio-economic and infrastructural components of resilience.

2.5 Empirical weighted equation

This method aims to calculate the snow hazard index, representing the impact level of a snowstorm (China Meteorological Administration 2021). The equation is presented as follows:

$$SH = IR + IRM + ID + IN + IT + IW + IRH$$

Where, SH represents the snow hazard index; I_R is accumulated snowfall (mm); I_{RM} denotes maximum daily snowfall (mm); I_D indicates snow depth (cm); I_N represents consecutive days with snowfall (d); I_T is daily minimum air temperature; I_W denotes the daily maximum wind speed (m/s); I_{RH} represents the daily minimum relative humidity (%).

Table 2 Indicators used to assess snowstorm resilience across multiple dimensions

Dimension	First-level indicators	Second-level indicators	References
Snow Hazard (SH)	Meteorological conditions	Accumulated snowfall (mm)	(China Meteorological Administration 2021)
		Number of consecutive days with snowfall (d)	
		Maximum daily snowfall (mm)	
		Snow depth (cm)	
		Daily maximum wind speed (m/s)	
		Daily minimum air temperature (°C)	
		Daily minimum relative humidity (%)	
Exposure (E)	Social economic conditions	Per Capita GDP (CNY/person)	(Wang et al. 2019)
		Total social fixed asset investment per km² (CNY/km²)	(Wang et al. 2019)
	Population conditions	Urban Population Density (person/km²)	(Aksha and Emrich 2020)
	Land conditions	Construction land area, % total area	(Germain 2016)
	infrastructure conditions	Total social electricity consumption (kWh)	(Pitto et al. 2019)
Vulnerability (V)	Social economic conditions	Agricultural Added Value (CNY)	
		Livestock Added Value (CNY)	(Wang et al. 2019)
		Number of workers in agriculture, forestry, animal husbandry and fisheries, % urban population	(Aksha and Emrich 2020)
	Population conditions	Proportion of children	(Cai et al. 2018)
		Proportion of elder people	(Cai et al. 2018)
	Land conditions	Proportion of commonly used arable land relative to total land area	
		Proportion of total area sown with crops	
		Proportion of grassland within the total land area	(Wang et al. 2019)
	infrastructure conditions	Residential Electricity Consumption in urban and rural areas	(Carlini et al. 2019)
Adaptive capability (A)	Communication system	Proportion of households with fixed telephone subscriptions relative to urban population	(Aksha and Emrich 2020)
		Proportion of households with mobile telephone subscriptions relative to urban population	(Aksha and Emrich 2020)
		Proportion of households with broadband access subscriptions relative to urban population	(Aksha and Emrich 2020)
	Health system	Proportion of hospital and health center beds to urban population	(Cai et al. 2018)
		Proportion of health technicians in hospitals and health centers relative to urban population	(Cai et al. 2018)
		Proportion of licensed physicians in hospitals and health centers relative to urban population	(Cai et al. 2018)
	Transportation system	Railway Network Density(km/km²)	(J. Wang and Liu 2019)
		Intercity Expressway Density(km/km²)	(J. Wang and Liu 2019)
		Urban Road Network Density(km/km²)	(J. Wang and Liu 2019)

2.6 Entropy weight method

This method aims to minimize subjectivity in weight allocation. Given the time-series data, it is assumed that the assigned weights for these indicators remain stable. To accommodate this, an exponential decay model was applied to dynamically adjust past weights. The detailed procedures of the entropy method are outlined as follows: (Xu and Yang 2024):

(1) Standardize indicator values: Transform each indicator to a value between 0 and 1 using:

$$V_{norm} = (V_{init} - V_{min})/(V_{max} - V_{min})$$

Where, V_{norm} is the normalized value, V_{init}, V_{max} and V_{min} are the initial, maximum, and minimum values, respectively.

(2) Calculate proportion: For each indicator *j* and land patch *i*:

$$P_{tij} = V_{tij} / \sum_{i=1}^{m} V_{tij}$$

(3) Determine entropy: The entropy E_{tj} of each indicator i is:

$$E_{tj} = -ln\,(m) \sum {}^{m}_{i=1} P_{tij} ln\,(P_{tij})$$

Where *m* is the total number of land patches.

(4) Calculate entropy weights: The weight W'_{tj} is given by:

$$W'_{tj} = (1 - E_{tj})/(m - \sum_{i=1}^{m} E_{tj})$$

.

(5) Adjust weights over time: The exponential decay model refines the weights:

$$W_{tj} = W'_{tj} + W'_{(t-1)j} \cdot e^{-\Delta t}$$

Where, W_{tj} is the weight at time *t*, W'_{tj} and $W'_{(t-1)j}$ is the original weight at time *t*, *t* – 1, respectively.

2.7 Generalized linear model (GLM) model

GLM was employed to examine the relationship between snowstorm risk and disaster loss, incorporating variables such as affected population, impacted cropland area, and direct economic loss. Given the non-normal distribution of disaster loss data, a GLM with a Gamma family distribution was selected, which is appropriate for continuous, positively skewed response variables. The inverse power function was applied as the link function, allowing for a more flexible relationship between predictor and response variables. This configura-

tion provided a good model fit and captured key data patterns. Model fit was assessed using Pseudo R^2 and Pearson χ^2. The model can be formulated as follows:

$$g\left(E\left[Y\middle|x\right]\right) = \beta_0 + \beta_1 x$$

where, Y is the response variable (e.g., affected population, direct economic loss, or affected cropland area); x is the independent variable, representing snowstorm risk; β_0 is the intercept; β_1 is the risk coefficient; $g(.)$ denotes the inverse power link function.

2.8 Getis-Ord Gi* (Local G) analysis

The Getis-Ord Gi* (Local G) analysis was applied to identify hot and cold spots across various spatial dimensions. This method was selected for its capacity to reveal statistically significant spatial spot patterns, specifically pinpointing areas with high (hot spots) or low (cold spots) values relative to their neighboring locations. The Getis-Ord Gi* statistic computes a z-score and a p-value for each location, offering insights into the statistical significance and intensity of spot in the data. The z-score quantifies the extent to which the observed value deviates from the expected value in a random distribution, aiding in determining the statistical significance of the spot pattern. A high positive z-score indicates a hot spot, where high values are spatially clustered, while a low negative z-score indicates a cold spot, where low values are clustered. The formula for calculating the z-score in the Getis-Ord Gi* statistic is as follows:

$$z\left(Gi^*\right) = \left(Gi^* - E\left(Gi^*\right)\right) / \sqrt{Var\left(Gi^*\right)}$$

Where, Gi^* represents the observed Getis-Ord statistic for a location.

2.9 Time series k-means clustering

Time series k-means clustering was employed to identify temporal patterns across various dimensions, utilizing the unique structure of time-series data to reveal underlying trends and similarities over time. The Dynamic Time Warping technique was implemented to enhance clustering performance by aligning temporal sequences based on shape similarity rather than exact time points. The time series k-means algorithm iteratively assigns each time-series data point to one of k clusters by minimizing within-cluster variance, effectively adapting to temporal dependencies and seasonality within the data. The objective function for time series k-means is formulated as:

$$J = \sum_{i=1}^{k} \sum_{j=1}^{n_i} \left|\left| x_j^{(i)} - \mu_i \right|\right|^2$$

where J is the objective function representing the total within-cluster variance, k is the number of clusters, n_i is the number of time-series data points in cluster i, $x_j^{(i)}$ is the j-th time-series data point in cluster i, and μ_i is the centroid of cluster i.

2.10 Shapley additive explanations(SHAP)

SHAP analysis was applied to identify the primary drivers of snowstorm resilience by leveraging its interpretive capacity on a Gradient Boosting Machine (GBM) model. The GBM model was chosen for its high predictive performance and its capability to capture complex nonlinear relationships in data, making it especially well-suited for resilience prediction. GBM iteratively constructs a series of decision trees, with each subsequent tree addressing the residuals of the previous ones, thereby enhancing overall accuracy and robustness in capturing patterns that contribute to snowstorm resilience.

The SHAP method was used to interpret the GBM model's predictions, offering a mathematically grounded and intuitive approach to explaining complex models. Drawing on cooperative game theory, SHAP assigns each feature a Shapley value that quantifies its contribution to a specific prediction. This approach enables the decomposition of the GBM model's predictions into contributions from each feature, thereby identifying the most influential factors driving resilience outcomes.

3 Result

3.1 The correlation between snowstorm risk and actual disaster losses

Figure 3 depicts the temporal evolution of snowstorm risk assessment and its actual impacts in Heilongjiang Province from 2010 to 2019. This assessment is derived from various previously mentioned indicators, while the actual impacts are measured using indicators such as affected population, impacted cropland area, and direct economic losses, as recorded by the Heilongjiang Province Statistics Bureau. Each indicator exhibits a similar pattern of fluctuation over time, suggesting a potential correlation among them. The peak across all variables in 2012 likely indicates a particularly severe snowstorm event during that year. A slight increase in some variables is observed around 2018.

The GLM model was used to explore potential correlations between snowstorm risk and its impacts. Table 3 presents the results of a GLM statistical analysis examining the relationship between snowstorm risk (independent variable) and three impact indicators: affected population, direct economic loss, and affected cropland area. All models adopt an inverse

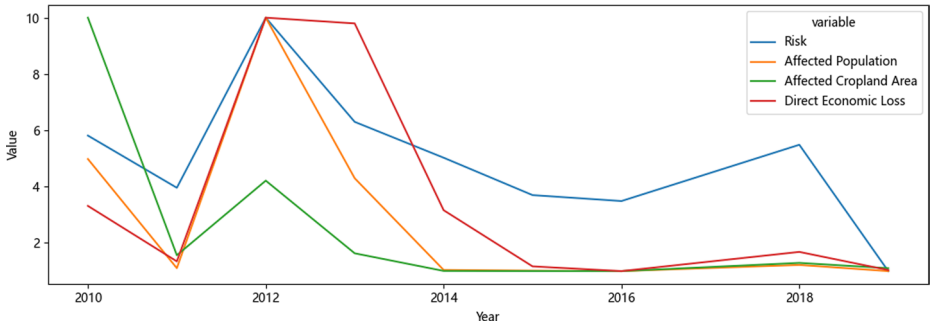

Fig. 3 Temporal evolution of snowstorm risk and its impacts on affected population, cropland area, and direct economic loss from 2010 to 2019

Table 3 GLM results for relationships between snowstorm risk and impact indicators

Model	Dependent Variable	Risk Coefficient (β_1)	Intercept (β_0)	Link Function	Pseudo R^2	Pearson χ^2
GLM 1	Affected Population	-0.09***	0.97***	Inverse power	0.7341	3.00
GLM 2	Direct Economic Loss	-0.05**	0.64***	Inverse power	0.5713	1.24
GLM 3	Affected Cropland Area	-0.06*	0.77***	Inverse power	0.3310	2.15

Note: β_1 represents the coefficient of the snowstorm risk variable; β_0 is the model intercept. ***$p<0.001$; **$p<0.01$; *$p<0.05$

power link function, which transforms the relationship between the linear predictor and the expected outcome. Due to the nature of the inverse function, a negative coefficient reflects a positive association between snowstorm risk and the magnitude of impact. The models show that higher snowstorm risk is significantly associated with greater impacts.

Specifically, GLM 1 for affected population shows the strongest inverse relationship with snowstorm risk (coefficient = -0.09, $p<0.001$), supported by a high pseudo R^2 value of 0.8823, suggesting that this model explains a substantial proportion of the variance. The model for direct economic loss (GLM 2) demonstrates a smaller yet statistically significant negative relationship with snowstorm risk (coefficient = -0.05, $p<0.01$), with a pseudo R^2 of 0.7011, indicating moderate explanatory power. The model for affected cropland area (GLM 3) presents the weakest, though still statistically significant, relationship (coefficient = -0.06, $p<0.05$), with the lowest pseudo R^2 value of 0.4214. This result suggests that snowstorm risk has comparatively limited explanatory power for agricultural impacts in Heilongjiang Province.

These results indicate that snowstorm risk affects each sector differently. The affected population appears most directly influenced by snowstorm risk, suggesting higher vulnerability or exposure of human populations to snowstorm events. Direct economic losses, while also impacted, show more moderate sensitivity, indicating that financial repercussions are influenced by snowstorm severity but may also depend on other economic resilience factors.

3.2 Spatial pattern of snowstorm resilience

Figure 4 presents the spatial distribution and spots of snowstorm resilience across Northeast China from 2005 to 2019, derived from the HEVA model combined with the Getis-Ord Gi* (Local G) analysis.

The top row shows resilience in 2005, 2010, 2015, and 2019, with blue-green indicating high and red indicating low values. In 2005, resilience is generally low, with substantial regions exhibiting low to medium-low resilience, notably concentrated in southern Heilongjiang, central Jilin, and widespread areas of Liaoning. By 2010, marginal improvements emerge, particularly in parts of central and eastern Heilongjiang and eastern Jilin. In 2015, resilience visibly increases, with more areas classified as medium to medium-high resilience. By 2019, a substantial shift is evident, as broader regions, especially in eastern Heilongjiang and central Jilin, display medium to high resilience levels.

The lower row of subplots demonstrates the hot and cold spot analysis based on the Getis-Ord Gi* statistic, which identifies statistically significant resilience spots. Spot intensity is indicated by z-scores, where higher (redder) and lower (bluer) z-scores signify stronger spot of low and high resilience, respectively. In 2005, cold spots are concentrated in

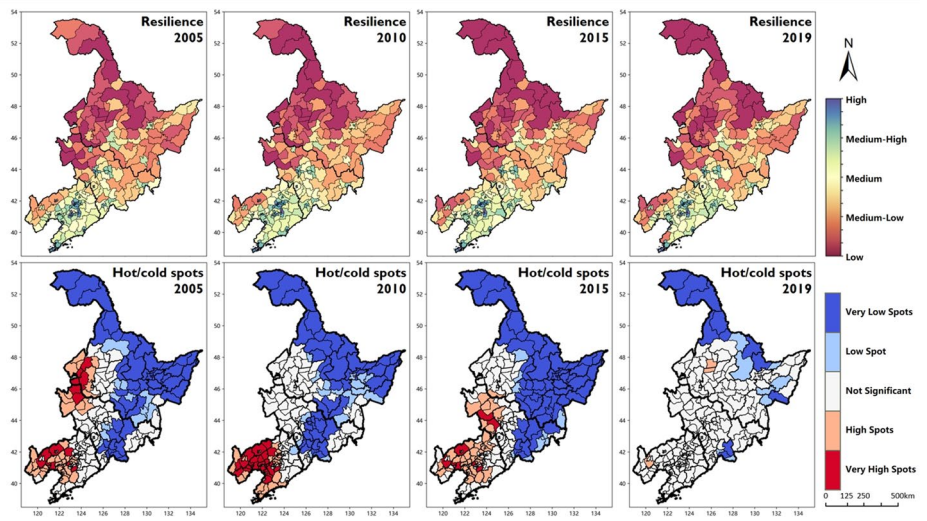

Fig. 4 Spatial distribution and hot/cold spot patterns of resilience in Northeast China from 2005 to 2019. (Top row: resilience levels over time; bottom row: spatial spot patterns of resilience)

northern Heilongjiang and central Jilin, while hot spots predominate in western Liaoning and southern Jilin. By 2010, cold spots extend across Heilongjiang, reflecting enhanced resilience in these regions, while hot spots persist in western Liaoning. In 2015, cold spots grow more prominent in northern and central Heilongjiang and spread into eastern Jilin, whereas hot spots decline in both extent and intensity. By 2019, cold spots further expand, encompassing nearly all of Heilongjiang and central Jilin, while hot spots diminish, limited to small areas in southern Liaoning.

These maps show a clear trend of increasing resilience across Northeast China over time. Initially, the region exhibits a mix of low to medium resilience, dispersed across northern and eastern Heilongjiang and central Jilin. Resilience improved over time, especially in northern and eastern Heilongjiang and Jilin by 2019. Conversely, resilience remains weaker in western and southern Liaoning, as indicated by persistent yet gradually diminishing hot spots.

This spatial pattern of resilience aligns closely with regional climatic gradients. As shown in Fig. 1, snow cover duration increases progressively from south to north, with southern Liaoning experiencing 0–30 snow cover days annually, while northern Heilongjiang sees up to 180–240 days. This climatic gradient significantly influences both hazard frequency and adaptive behavior. Regions with longer snow cover durations—particularly Heilongjiang and northern Jilin—have historically been more exposed to snow-related disruptions. However, urban clusters in these areas also appear to have developed stronger adaptive capacities over time, likely due to institutional familiarity with winter hazards and the integration of snow-resilient infrastructure. In contrast, southern Liaoning—where snowfall is more intermittent and less severe—shows weaker resilience, potentially due to a combination of high exposure and limited preparedness. These findings suggest that climatic characteristics, particularly the persistence of snow cover, may influence both the urgency and the long-term development of localized resilience strategies.

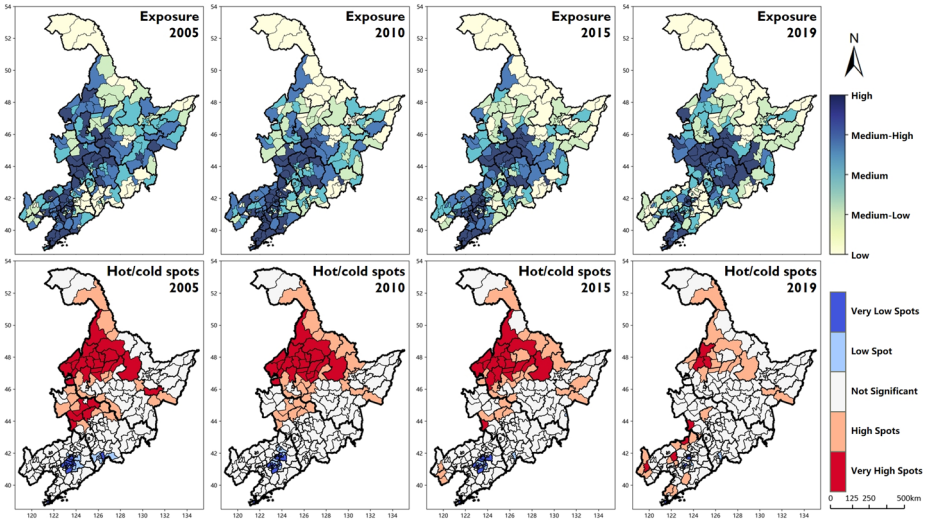

Fig. 5 Spatial distribution and hot/cold spot patterns of exposure in Northeast China from 2005 to 2019. (Top row: exposure levels over time; bottom row: spatial spot patterns of exposure)

Figure 5 is organized with the top row illustrating exposure levels across Northeast China and the bottom row highlighting the spatial spot of exposure. In the top row, exposure levels are shown from high (dark blue) to low (light green). In 2005, high exposure areas are scattered, notably in western and southern Heilongjiang, eastern Jilin, and parts of central Liaoning. By 2010, high exposure expands, especially in southern Heilongjiang and central Jilin, with Liaoning reaching medium to medium-high levels. In 2015, these zones intensify in central Heilongjiang and eastern Jilin, and by 2019, exposure remains high in southwestern Heilongjiang and central Jilin, though eastern Liaoning sees a slight decline.

The bottom row presents the hot and cold spot analysis, indicating spot intensity. In 2005, hot spots are centered in southern and western Heilongjiang and southwestern Jilin, with minimal cold spots in northern Heilongjiang. By 2010, hot spots intensify and spread into central Jilin, while cold spots emerge in northern Jilin. In 2015, hot spots persist in southern Heilongjiang and central Liaoning, with cold spots in northern Heilongjiang and eastern Jilin. By 2019, hot spots in central and southern Heilongjiang and parts of Jilin, with a slight decrease in Liaoning.

This spatial-temporal analysis highlights a trend of persistently high exposure in Heilongjiang and Jilin, where spot intensifies. Over time, these high-exposure areas broaden, especially in central Heilongjiang and Jilin, likely due to socio-economic factors, geographic vulnerability, or limited adaptation strategies.

Figure 6 examines the spatial-temporal evolution and spot of vulnerability levels across Northeast China, specifically within Heilongjiang, Jilin, and Liaoning provinces, from 2005 to 2019. The upper row of subplots depicts vulnerability levels, ranging from high (dark green) to low (light yellow). In 2005, high vulnerability areas are mainly located in western and southern Heilongjiang, central Jilin, and scattered parts of central and southern Liaoning. By 2010, these zones intensify in western Heilongjiang and central Jilin, while some areas in southern Liaoning show reduced vulnerability. In 2015, high vulnerability further

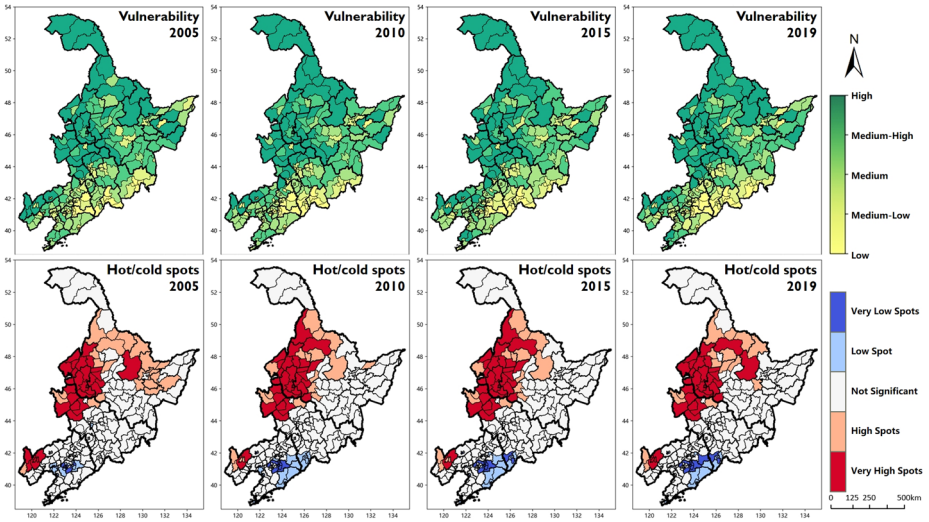

Fig. 6 Spatial distribution and hot/cold spot patterns of vulnerability in Northeast China from 2005 to 2019. (Top row: vulnerability levels over time; bottom row: spatial spot patterns of vulnerability)

spreads in central Heilongjiang and parts of eastern Jilin. By 2019, southern Liaoning shows a slight decline in vulnerability, though high levels persist in central Heilongjiang and Jilin.

The lower row displays the hot and cold spot analysis. In 2005, hot spots—indicating high vulnerability—are concentrated in southern Heilongjiang, central Jilin, and southwestern Liaoning, while cold spots are limited to isolated areas in eastern Heilongjiang. By 2010, hot spots expand across western Heilongjiang and central Jilin, and cold spots emerge in northeastern Jilin and eastern Liaoning. In 2015, hot spots remain prominent in central Heilongjiang and Jilin, with cold spots more visible in eastern Jilin and southwestern Liaoning. By 2019, high-vulnerability hot spots remain centered in central Heilongjiang and Jilin, while Liaoning sees a slight decrease in intensity; cold spots persist in eastern Jilin.

This analysis highlights persistently high or increasing vulnerability in regions such as central Heilongjiang and Jilin, where vulnerability intensifies over time, possibly due to environmental or socio-economic factors. Meanwhile, certain areas in Liaoning show reduced vulnerability by 2019, likely reflecting effective risk mitigation efforts.

Figure 7 depicts the spatial distribution and spot of adaptive capacity across Northeast China from 2005 to 2019. In the upper row, adaptive capacity is shown from high (dark orange) to low (light yellow). Initially, in 2005, capacity is generally low to medium, with higher levels scattered in central Jilin and parts of Liaoning. By 2010, slight improvements appear in northern Heilongjiang and eastern Jilin, though most areas remain at medium to medium-low levels. In 2015, adaptive capacity strengthens further, especially in northern and eastern Heilongjiang, and by 2019, there is a notable increase across northern Heilongjiang and eastern Jilin, reflecting steady regional improvement.

The lower row presents hot and cold spot analysis. In 2005, cold spots (higher adaptive capacity) are sparse, mainly in northern Heilongjiang, while hot spots (lower capacity) are concentrated in southern Liaoning. By 2010, cold spots expand in northern Heilongjiang, indicating improvement, while hot spots decrease in intensity. This trend continues in 2015,

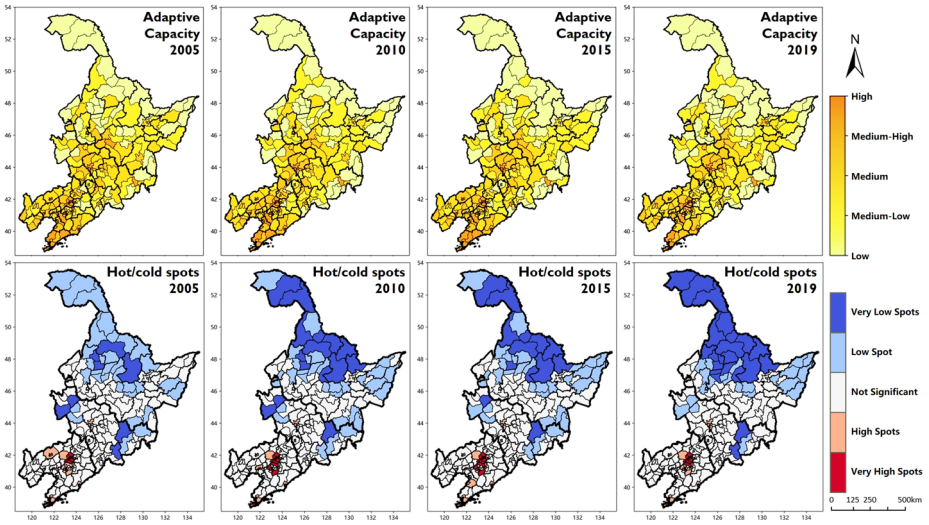

Fig. 7 Spatial distribution and hot/cold spot patterns of adaptive capacity in Northeast China from 2005 to 2019. (Top row: adaptive capacity levels over time; bottom row: spatial spot patterns of adaptive capacity)

with cold spots spreading to eastern Jilin and hot spots diminishing in Liaoning. By 2019, cold spots cover much of Heilongjiang, and hot spots have nearly vanished.

Overall, adaptive capacity shows a positive trend, with sustained improvement over time, particularly in Heilongjiang and Jilin, likely due to effective adaptation measures.

3.3 Temporal clustering of snowstorm resilience

The Fig. 8 shows the silhouette scores used to determine the optimal number of clusters in time-series resilience analysis. Silhouette scores decline with more clusters, stabilizing at five. This stabilization suggests that five clusters provide the optimal balance, as additional clusters do not significantly enhance cohesion or separation.

The Fig. 9 illustrates the temporal and spatial patterns of snowstorm resilience across Northeast China from 2005 to 2019, segmented into distinct clusters based on three core dimensions: adaptive capacity, vulnerability, and exposure. The identified clusters reflect distinct resilience trajectories across regions.

Cluster 0, in northwestern Heilongjiang, exhibits the lowest resilience, driven by minimal adaptive capacity, high vulnerability, and increasing exposure—highlighting an urgent need for targeted interventions. Clusters 1 and 2 show moderate resilience, with relatively stable vulnerability and slow gains in adaptive capacity. While exposure continues to rise in Cluster 1, Cluster 2 shows a slight decline, possibly due to local adaptation measures. Cluster 3, located in southern and western Liaoning, demonstrates improved resilience over time, supported by low vulnerability and gradually increasing adaptive capacity. Cluster 4, centered on provincial capitals, has the highest adaptive capacity and lowest vulnerability among all clusters, though increasing exposure remains a concern.

Overall, this analysis reveals a diverse landscape of snowstorm resilience across Northeast China, with varying levels of adaptive capacity, vulnerability, and exposure. Regions

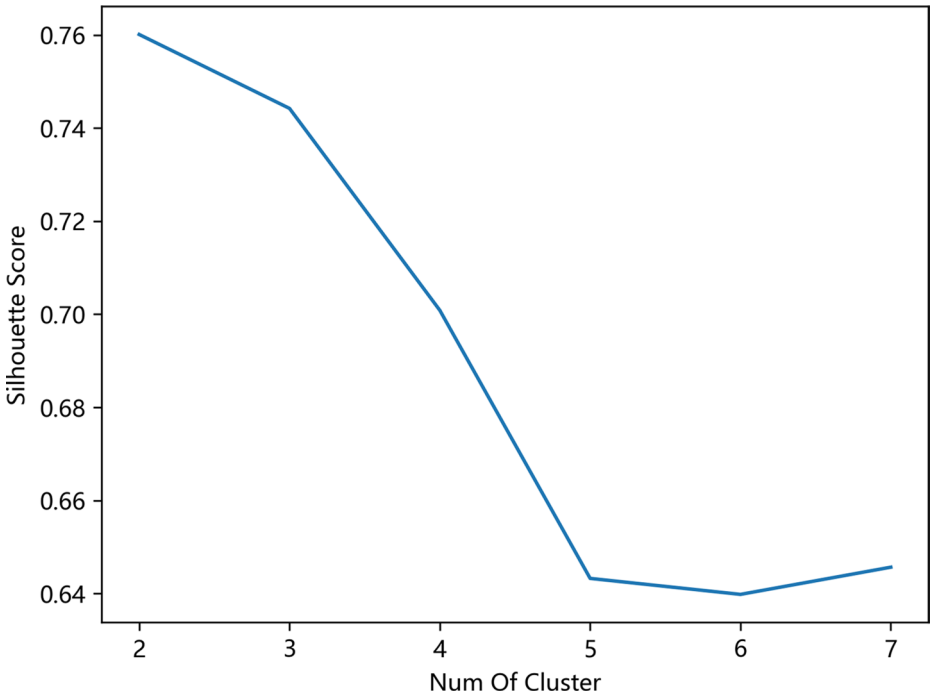

Fig. 8 Silhouette scores for determining the optimal number of clusters in time series resilience analysis

with high adaptive capacity and low vulnerability, such as central Liaoning (Cluster 4), are generally more resilient. Conversely, areas like northwestern Heilongjiang (Cluster 0) remain highly susceptible to snowstorm impacts, underscoring a need for enhanced resilience measures. This analysis highlights both strengths and challenges, offering a basis for targeted policy actions.

3.4 Influence factor of snowstorm resilience

The GBM model was used to analyse snowstorm resilience across various regions by incorporating multiple indicators. The model demonstrates strong predictive accuracy, with a Mean Squared Error (MSE) of 0.000119 and a Root Mean Squared Error (RMSE) of approximately 0.0109 on the test data. The low errors suggest that the GBM model captures regional resilience patterns effectively.

The SHAP summary plot, displayed in Fig. 10, illustrates the contribution of various features to the model's predictions. Features with higher SHAP values have a stronger influence on the model's output. Among these, Urban Road Network Density, Grassland Coverage, and Intercity Expressway Density are the most influential factors, with positive SHAP values suggesting they contribute to higher resilience. This indicates that areas with well-developed infrastructure and extensive grassland coverage are likely to exhibit greater resilience to snowstorms, as these features provide economic stability and serve as environmental buffers against extreme weather.

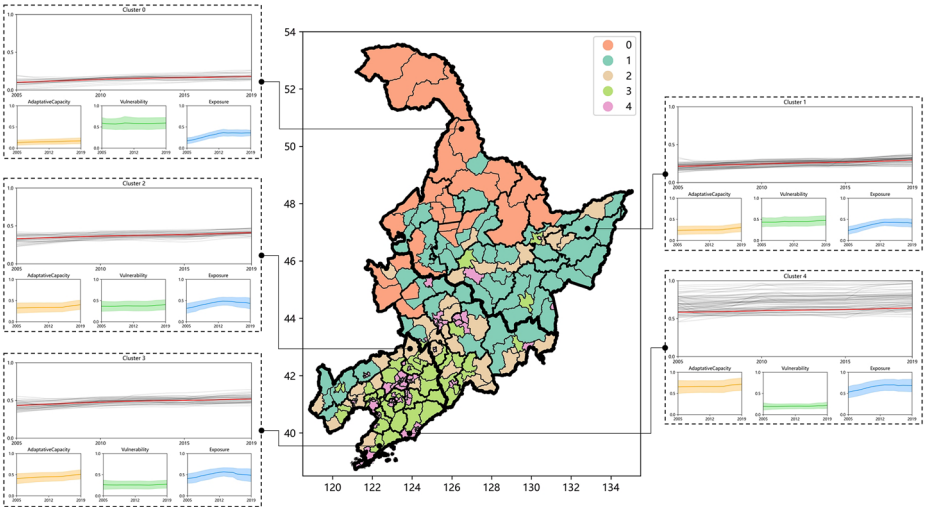

Fig. 9 Temporal patterns of snowstorm resilience across clusters in Northeast China, with adaptive capacity, vulnerability, and exposure trends for each cluster from 2005 to 2019

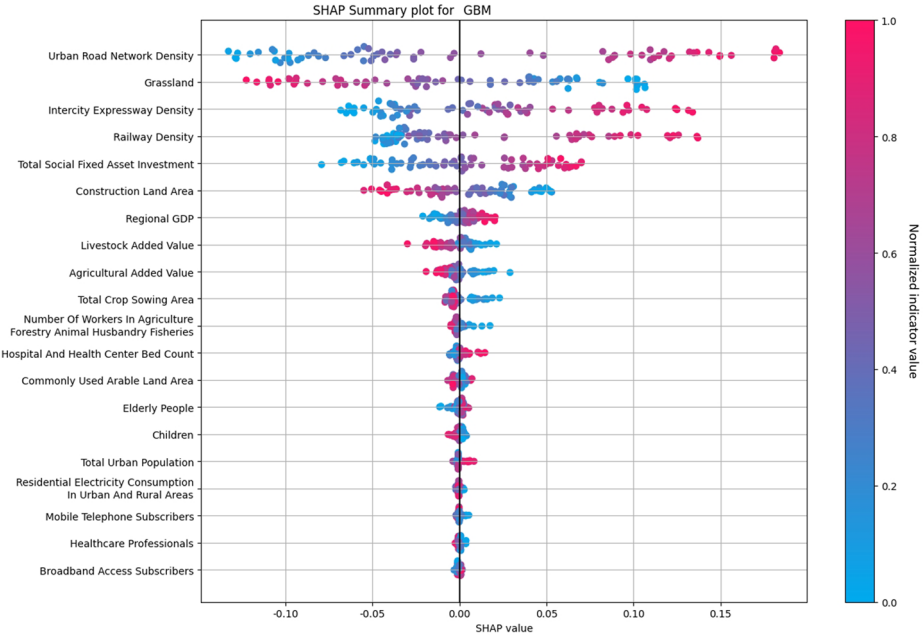

Fig. 10 SHAP summary plot for the GBM model, showing the impact of various indicators on snowstorm resilience predictions

The permutation importance plot in Fig. 11, supports these findings by ranking features based on their impact on the model's predictive accuracy. Grassland Coverage has the highest relative importance at 0.1025 (18.9%), followed closely by Intercity Expressway Density at 0.0916 (16.9%) and Urban Road Network Density at 0.0875 (16.2%). These

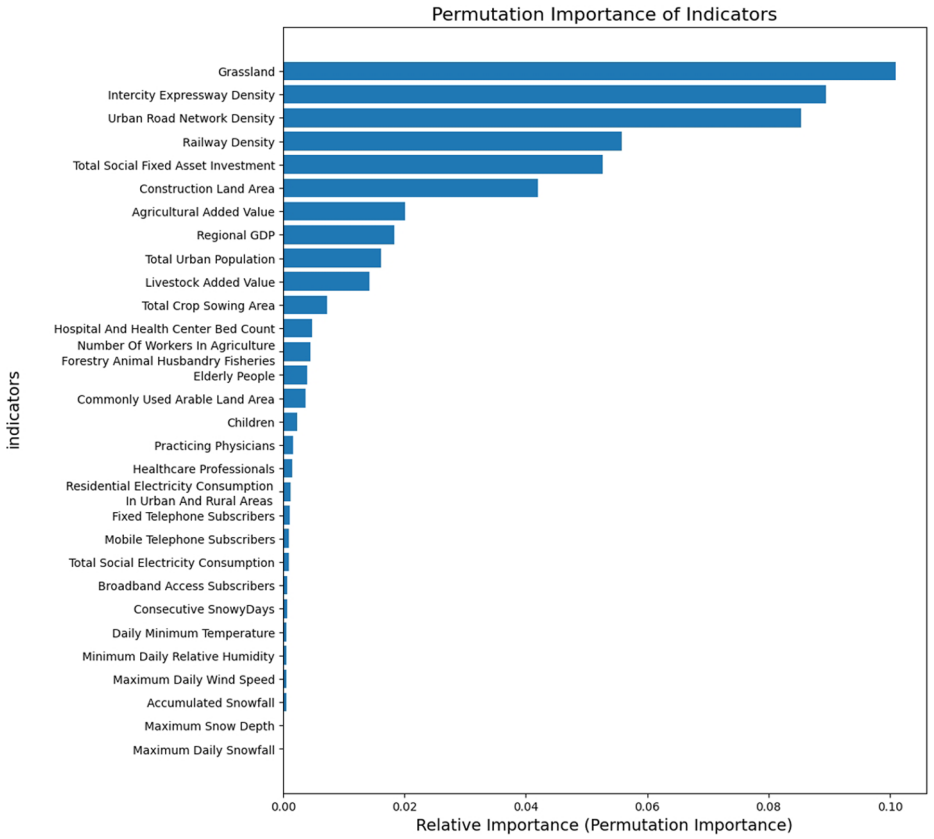

Fig. 11 The permutation importance of indicators of GBM

infrastructure-related factors are critical as they enhance accessibility and connectivity, which aid in faster responses to snowstorms and facilitate efficient resource distribution during such events. Other features, such as Railway Density and Total Social Fixed Asset Investment, also demonstrate significant importance, underscoring the role of economic and transportation infrastructure in strengthening resilience.

These analyses highlight critical infrastructure and environmental factors that significantly enhance snowstorm resilience across Northeast China. Urban Road Network Density, Grassland Coverage, and Intercity Expressway Density emerge as the most influential features. These features improve connectivity and speed emergency response. Grasslands act as natural buffers, adding environmental stability. Other important factors, such as Railway Density and Total Social Fixed Asset Investment, further underscore the importance of robust transportation and economic infrastructure in disaster preparedness. These findings suggest that prioritizing the development of resilient infrastructure, expanding green spaces, and investing in economic assets are beneficial adaptation measures that can substantially mitigate the adverse effects of snowstorms and strengthen regional resilience.

4 Discussion

4.1 The urgency of snow disaster resilience research

With the intensification of global climate change, the frequency and severity of extreme natural disasters are escalating worldwide. Snow disasters in mid- to high-latitude regions are no exception. According to IPCC Sixth Assessment Report (2021), while overall snowfall may decrease, the intensity and frequency of heavy snow events are projected to rise in certain regions due to increased atmospheric moisture content (Masson-Delmotte et al. 2021). O'Gorman (2014) found that extreme snowfall could become more frequent in colder regions despite a decrease in average snowfall.

Furthermore, snow disasters often have more severe impacts than other forms of precipitation-related events. Heavy snowfall can lead to infrastructure collapse, transportation paralysis, and power outages, exacerbating human casualties and economic losses. The 2008 snow disaster in southern China serves as a stark example, where prolonged snowfall directly impacted more than 100 million people and resulted in economic losses exceeding $21 billion(Gao 2016). Unlike heavy rain, snow's prolonged presence and the subsequent melting process can cause extended disruptions.

Therefore, strengthening resilience across mid- to high-latitude regions is essential for mitigating the future risks of snow disasters. Our study has several concrete implications for infrastructure planning, spatial policy, and disaster risk management in high-latitude regions.

First, the temporal clustering analysis (Fig. 9) can assist policymakers in prioritizing intervention zones. For example, Cluster 0—characterized by persistently low resilience and increasing exposure in northwestern Heilongjiang—could be prioritized for investments in adaptive infrastructure such as resilient power grids, and early warning systems. Notably, this cluster is concentrated in rural areas, which often face structural disadvantages not fully captured by indicator data. These include limited fiscal capacity, underdeveloped infrastructure, and insufficient disaster preparedness mechanisms compared to urban regions. The institutional lag in implementing snow-related disaster risk reduction measures may further exacerbate vulnerability and hinder resilience-building in these regions. Second, the spatial hot and cold spot maps (Figs. 4, 5, 6 and 7) offer a visual decision-support tool for targeting spatially uneven resilience. Cold spots of adaptive capacity, such as those found in southern Liaoning, indicate areas where medical, transport, or communication systems may require upgrades to withstand future snow hazards. Third, the SHAP analysis (Fig. 10) highlights the most influential features driving resilience, such as urban road density, grassland coverage, and intercity expressway infrastructure. These findings can directly inform infrastructure investment priorities.

4.2 Transition in snowstorm disaster research

The study of snowstorm disasters is undergoing a significant transformation toward more advanced, integrative, and quantitative approaches. Historically, research in this field was predominantly qualitative, focusing on descriptive analyses without robust empirical underpinnings. Recently, however, the focus has shifted toward quantifying vulnerability and

resilience through statistical models and data-driven techniques, marking a pivotal advancement in research.

In terms of quantitative methods, advanced machine learning techniques are now employed to identify time series patterns and uncover the driving forces behind snowstorm disasters. These models enable the handing of large, complex datasets and capture nonlinear relationships between variables that traditional statistical methods might overlook (Pichler and Hartig 2023). This improves prediction and clarifies drivers of vulnerability and resilience.

Moreover, this research utilizes a comprehensive spatiotemporal dataset spanning 15 years (2005–2019) across Northeast China. This extensive dataset enables a nuanced analysis of temporal trends and spatial patterns, surpassing the scope of previous studies that often focused on shorter time frames or limited regions (Mirjalili et al. 2023).

This research perspective is also exceptionally comprehensive. We examine a broad array of factors, including social, economic, environmental, land use, transportation, healthcare, and communication systems. By integrating these diverse elements, we aim to provide a holistic assessment that can inform more effective mitigation and adaptation strategies. Contemporary studies advocate for integrated analyses across social, economic, environmental, and infrastructural systems, often within the context of typhoon disasters (Z. Wang et al., 2024). However, this holistic approach to snowstorm disaster resilience underscores the understanding that resilience arises from the interconnectedness of multiple systems rather than from isolated components.

4.3 Framework applicability and limitations

While the HEVA framework demonstrates flexibility through the integration of data-driven techniques such as entropy weighting, GLM, and machine learning algorithm, its transferability to other regions or hazards may be constrained by data availability. The framework relies heavily on high-resolution, long-term spatial and temporal datasets across multiple dimensions, including hazard characteristics, exposure, vulnerability, and adaptive capacity. In contexts where such datasets are incomplete, inconsistent, or unavailable—particularly in low-resource or data-scarce regions—replicating the framework in its full form may be difficult. For example, indicators such as population disaggregation, infrastructure capacity, and land-use change often require harmonized administrative and geospatial sources, which are not uniformly accessible across countries or regions.

Moreover, the applicability of the HEVA framework to other types of hazards depends on the maturity of domain-specific hazard modeling and prediction techniques. This study benefited from the availability of gridded snow hazard datasets (e.g., snow water equivalent, snow cover days), which are critical for capturing seasonal dynamics and historical risk. However, in the case of compound, short-duration, or emerging hazards, methodological transfer may be limited unless suitable hazard metrics and predictive models are developed. Thus, future work should emphasize improving data infrastructures and hazard-specific methodologies to enhance the adaptability of the HEVA framework in diverse contexts.

5 Conclusion

This study provides an indicator-based framework to assess snowstorm resilience in Northeast China, addressing a key gap in high-latitude research. By employing the HEVA model and integrating advanced machine learning techniques, we analysed the spatiotemporal evolution of snowstorm resilience across Heilongjiang, Jilin, and Liaoning provinces from 2005 to 2019.

Our findings reveal a significant correlation between snowstorm risk and actual disaster losses, validating the effectiveness of the HEVA model. Spatial analysis indicates a general improvement in resilience over time, especially in northern and eastern Heilongjiang and central Jilin, though notable regional disparities persist. Temporal clustering identified distinct resilience patterns, influenced by factors such as infrastructure development, economic resources, and land use. Specifically, regions with higher infrastructure density and grassland coverage demonstrated greater resilience, underscoring the importance of these factors in mitigating snowstorm impacts.

The study underscores the urgency of enhancing snow disaster resilience in the face of increasing extreme weather events due to climate change. By highlighting the roles of key adaptation measures—such as expanding transportation networks, maintaining environmental buffers like grasslands, and investing in economic assets—this research offers actionable insights for building resilience in snowstorm-prone regions. The framework supports policymakers in assessing and improving resilience across space and time, equipping them with practical strategies for reducing vulnerability.

Future research should focus on refining the framework by incorporating additional variables and exploring its applicability in other high-latitude regions facing similar challenges. Overall, this study contributes a robust knowledge base for understanding and improving snow disaster resilience, aiding informed decision-making and policy formulation aimed at mitigating the impacts of snowstorms in vulnerable urban environments.

Supplementary Information The online version contains supplementary material available at https://doi.org/10.1007/s11069-025-07591-8.

Funding Open access funding provided by Politecnico di Torino within the CRUI-CARE Agreement. We acknowledge the financial support of the National Natural Science Foundation of China (grant numbers: 51761135025, 51778233), Guangdong Science and Technology Department (grant numbers: 2020B1010010002), China Postdoctoral Science Foundation (No: 2025M771604), and Postdoctoral Fellowship Program (Grade C) of China Postdoctoral Science Foundation (No: GZC20251107).

Data availability The raw data supporting the conclusions of this article will be made available by the authors on request.

Declarations

Conflict of interest The authors declare no conflicts of interest. The funders had no role in the design of the study; in the collection, analyses, or interpretation of the data; in the writing of the manuscript; or in the decision to publish the results.

References

Aksha SK, Emrich CT (2020) Benchmarking community disaster resilience in Nepal. International Journal of Environmental Research and Public Health, 17(6), 1985

Cai H, Lam NSN, Qiang Y, Zou L, Correll RM, Mihunov V (2018) A synthesis of disaster resilience measurement methods and indices. Int J Disaster Risk Reduct 31:844–855. https://doi.org/10.1016/j.ijdrr.2018.07.015

Carlini EM, Michi L, Rampazzo D, Marchesin A, Quaciari C, Geremia E, Quaia S (2019) Dispatching measures for improving the resilience of the Italian sub-transmission grid against ice and snow events. 2019 AEIT International Annual Conference (AEIT), 1–6. https://doi.org/10.23919/AEIT.2019.8893386

China Meteorological Administration (2021) Meteorological grades for urban snow hazard. No. GB/T, pp 40239–42021

Conroy G (2023) What the science says about california's record–setting snow. Nature. https://doi.org/10.1038/d41586-023-00937-x. d41586-023-00937–x

Ding Y, Yang J, Wang S, Chang Y (2021) A review of the interaction between the cryosphere and atmosphere. Sci Cold Arid Regions 12(6):329–342

Dong J, Peng J, He X, Corcoran J, Qiu S, Wang X (2020) Heatwave-induced human health risk assessment in megacities based on heat stress-social vulnerability-human exposure framework. Landsc Urban Plann 203:103907. https://doi.org/10.1016/j.landurbplan.2020.103907

Freddi F, Galasso C, Cremen G, Dall'Asta A, Di Sarno L, Giaralis A et al (2021a) Innovations in earthquake risk reduction for resilience: recent advances and challenges. Int J Disaster Risk Reduct 60:102267. https://doi.org/10.1016/j.ijdrr.2021.102267

Freddi F, Novelli V, Gentile R, Veliu E, Andreev S, Andonov A et al (2021b) Observations from the 26th November 2019 Albania earthquake: the earthquake engineering field investigation team (EEFIT) mission. Bull Earthq Eng 19(5):2013–2044. https://doi.org/10.1007/s10518-021-01062-8

Gao J (2016) Analysis and assessment of the risk of snow and freezing disaster in China. Int J Disaster Risk Reduct 19:334–340. https://doi.org/10.1016/j.ijdrr.2016.09.007

Germain D (2016) Snow avalanche hazard assessment and risk management in Northern quebec, Eastern Canada. Nat Hazards 80(2):1303–1321. https://doi.org/10.1007/s11069-015-2024-z

Haeberli W, Whiteman C (2021) Snow and ice-related hazards, risks, and disasters: Facing challenges of rapid change and long-term commitments. In Snow and Ice-Related Hazards, Risks, and Disasters (pp. 1–33). Elsevier. https://doi.org/10.1016/B978-0-12-817129-5.00014-7

He J, Duan W, Zhou Y, Su Y (2024) Impact of media information on social response in disasters: A case study of the Freezing-Rain and snowstorm disasters in Southern China in 2008. Int J Disaster Risk Sci 15(1):73–87. https://doi.org/10.1007/s13753-024-00539-9

Kawase H, Yamazaki T, Sugimoto S, Sasai T, Ito R, Hamada T et al (2020) Changes in extremely heavy and light snow-cover winters due to global warming over high mountainous areas in central Japan. Progress Earth Planet Sci 7(1):10. https://doi.org/10.1186/s40645-020-0322-x

Liu X, Hou K, Jia H, Zhao J, Mili L, Jin X, Wang D (2020) A Planning-Oriented resilience assessment framework for transmission systems under typhoon disasters. IEEE Trans Smart Grid 11(6):5431–5441. https://doi.org/10.1109/TSG.2020.3008228

Liu M, Patel VR, Wadhera RK (2025) Cold-Related deaths in the US. JAMA 333(5):427. https://doi.org/10.1001/jama.2024.25194

Masson-Delmotte V, Zhai P, Pirani S, Connors C, Péan S, Berger N, Caud Y, Chen L, Goldfarb M, Scheel Monteiro PM (2021) *Ipcc, 2021:* Summary for policymakers. In: Climate change 2021: The physical science basis. Contribution of working group i to the sixth assessment report of the intergovernmental panel on climate change

Miller JR, Fuller JE, Puma MJ, Finnegan JM (2021) Elevation-dependent warming in the Eastern Siberian Arctic. Environ Res Lett 16(2):024044. 10.1088/1748-9326/abdb5e

Mirjalili R, Barati H, Yazici A (2023) Resilience analysis of New York City transportation network after snow storms. Transport Res Record 2677(1):694-707

Morrison A, Westbrook CJ, Noble BF (2018) A review of the flood risk management governance and resilience literature. J Flood Risk Manage 11(3):291-304

Musselman KN, Lehner F, Ikeda K, Clark MP, Prein AF, Liu C, Barlage M, Rasmussen R (2018) Projected increases and shifts in rain-on-snow flood risk over Western North America. Nat Clim Change 8(9):808–812. https://doi.org/10.1038/s41558-018-0236-4

O'Gorman PA (2014) Contrasting responses of mean and extreme snowfall to climate change. Nature 512(7515):416–418. https://doi.org/10.1038/nature13625

Parker CL, Mooney PA, Webster MA, Boisvert LN (2022) The influence of recent and future climate change on spring Arctic cyclones. Nat Commun 13(1):6514. https://doi.org/10.1038/s41467-022-34126-7

Pichler M, Hartig F (2023) Machine learning and deep learning—a review for ecologists. Methods Ecol Evol 14(4):994-1016

Pitto A, Cirio D, Ciapessoni E, Pirovano G (2019) Analytical modeling of overhead line vulnerability to wet snow events for resilience assessment. 2019 AEIT International Annual Conference (AEIT), 1–6. https://doi.org/10.23919/AEIT.2019.8893309

Quante L, Willner SN, Middelanis R, Levermann A (2021) Regions of intensification of extreme snowfall under future warming. Sci Rep 11(1):16621. https://doi.org/10.1038/s41598-021-95979-4

Salas RN, Burke LG, Phelan J, Wellenius GA, Orav EJ, Jha AK (2024) Impact of extreme weather events on healthcare utilization and mortality in the united States. Nat Med 30(4):1118–1126. https://doi.org/10.1038/s41591-024-02833-x

Shah MAR, Renaud FG, Anderson CC, Wild A, Domeneghetti A, Polderman A, Votsis A, Pulvirenti B, Basu B, Thomson C, Panga D, Pouta E, Toth E, Pilla F, Sahani J, Ommer J, El Zohbi J, Munro K, Stefanopoulou M, Zixuan W (2020) A review of hydro-meteorological hazard, vulnerability, and risk assessment frameworks and indicators in the context of nature-based solutions. Int J Disaster Risk Reduct 50:101728. https://doi.org/10.1016/j.ijdrr.2020.101728

Shi Y, Zhai G, Xu L, Zhou S, Lu Y, Liu H, Huang W (2021) Assessment methods of urban system resilience: from the perspective of complex adaptive system theory. Cities 112:103141. https://doi.org/10.1016/j.cities.2021.103141

Walsh JE (2020) Arctic climate change, variability, and extremes. In: Arctic hydrology, permafrost and ecosystems. Springer International Publishing, Cham, pp 3–23. https://doi.org/10.1007/978-3-030-50930-9_1

Wang J, Liu H (2019) Snow removal resource location and allocation optimization for urban road network recovery: A resilience perspective. J Ambient Intell Humaniz Comput 10(1):395–408. https://doi.org/10.1007/s12652-018-0717-3

Wang S, Lanyue Z, Yanqiang W (2019) Integrated risk assessment of snow disaster over the Qinghai-Tibet plateau. Geomatics Nat Hazards Risk, 10(1)

Xu C, Yang L (2024) Evaluation of land resources carrying capacity based on entropy weight and cloud similarity. Sci Rep 14(1):9050. https://doi.org/10.1038/s41598-024-59692-2

Zhao T, Sun L (2021) Seismic resilience assessment of critical infrastructure-community systems considering looped interdependences. Int J Disaster Risk Reduct 59:102246. https://doi.org/10.1016/j.ijdrr.2021.102246

Authors and Affiliations

Peijun Lu[1] · Yicheng Wang[2]

✉ Yicheng Wang
yicheng.wang@polito.it

[1] School of Architecture, Tsinghua University, Haidian District, Beijing 100084, China

[2] Department of Architecture and Design, Politecnico di Torino, Torino 10125, Italy